Separation Science and Technology
Publication details, including instructions for authors and subscription information:
http://www.informaworld.com/smpp/title~content=t713708471

Calculation of Adsorption Bed Capacity by the Theory of Statistical Moments

Otto Grubner[a]; Dwight W. Underbill[a]
[a] SCHOOL OF PUBLIC HEALTH HARVARD UNIVERSITY BOSTON, MASSACHUSETTS

To cite this Article Grubner, Otto and Underbill, Dwight W.(1970) 'Calculation of Adsorption Bed Capacity by the Theory of Statistical Moments', Separation Science and Technology, 5: 5, 555 — 582
To link to this Article: DOI: 10.1080/00372367008055519
URL: http://dx.doi.org/10.1080/00372367008055519

SEPARATION SCIENCE, 5(5), pp. 555–582, October, 1970

Calculation of Adsorption Bed Capacity by the Theory of Statistical Moments

OTTO GRUBNER and DWIGHT W. UNDERHILL
SCHOOL OF PUBLIC HEALTH
HARVARD UNIVERSITY
BOSTON, MASSACHUSETTS 02115

Summary

Using the Statistical Moments Theory, a system of equations has been developed which provides a new approach to understanding dynamic gas adsorption. These equations describe adsorption breakthrough curves in a simple form which exhibits a close correlation between theory and published experiments. Because these equations are readily understood from a physical viewpoint, it is believed that they will not only help to clarify our concepts of dynamic adsorption, but will also improve our understanding of the physical meaning of what takes place in an adsorption bed.

1. BASIC CONCEPTS

The efficiency of mass transfer plays an important role in adsorption from moving gas streams. As a general rule, the amount of adsorbate retained by dynamic adsorption from a flowing gas stream is smaller than the amount corresponding to equilibrium conditions. To illustrate this effect, let us suppose that it is required to remove 90% of an undesired product from a gas stream. This permits an adsorption bed to be used until there is a breakthrough of 10% of the input concentration of the gas being removed. Figure 1 shows a distribution of the adsorbate across an adsorption bed. The over-all adsorption efficiency, calculated from the ratio of the amount of adsorbate actually retained on the bed to the amount of adsorbate required to fully saturate the bed, depends on the distribution of adsorbate across the bed at the time of breakthrough. As shown in this paper, the effects of this

a) Start of Adsorption Cycle

b) Midpoint of Adsorption Cycle

c) End of Adsorption Cycle
(Breakthrough)

d) Start of Adsorption Cycle

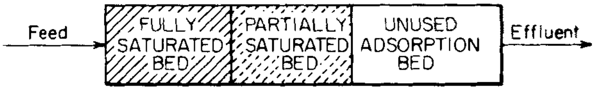

e) Midpoint of Adsorption Cycle

f) End of Adsorption Cycle
(Breakthrough)

FIG. 1. The effect of imperfect mass transfer on adsorption bed efficiency. Figures a–c illustrate adsorption under conditions of ideal mass transfer. The front of adsorbate in the bed remains sharp and feed can be passed into the adsorption bed until it is fully saturated. Figures d–f illustrate adsorption with nonideal mass transfer. In these figures the area of partial saturation represents adsorption bed volume which is effectively lost due to nonideal mass transfer; breakthrough occurs before the bed is fully saturated.

distribution can be calculated by the method of statistical moments (*1*). This new knowledge should lead to improvements in the design of adsorption processes for solvent recovery, air pollution abatement, removal of fission products, etc.

This paper will consider only the dynamic adsorption of gases on porous adsorbents. However, the theory is quite general and may apply as well to other separation processes, such as thin-layer chromatography and gas–liquid chromatography.

1.1. Some Basic Assumptions

Certain basic assumptions have been made:

1.1.1. The adsorption bed is cylindrical, with a length, L, and a cross-sectional area, Q.

1.1.2. The bed is evenly filled with spherical adsorbant particles having a diameter, $2R$. It is not necessary that the particles be spherical; calculations can be based on other absorbent particle shapes (*2*, *3*).

1.1.3. Wall effects are negligible. This requires that the bed diameter be at least 12 times greater than the particle diameter.

1.1.4. The fluid phase streams between the particles in a free volume defined as the interparticle void volume.

1.2. Definitions of Porosity

Precise definitions of porosity are vital to the concepts being discussed here. The interparticle void volume per unit volume of the adsorption bed is called the external porosity, ϵ_e. The external porosity is assumed to have the same value throughout the bed. The absorbent particles are also porous; in fact, each adsorbent particle can be conceived of as a conglomerate of many smaller particles. The fraction of void volume in each particle is also assumed to be a constant, denoted as β. In a unit volume of the adsorption bed, there are $(1 - \epsilon_e)$ units of volume occupied by the adsorbent particles and therefore $\beta(1 - \epsilon_e) = \epsilon_i$ units of intraparticle void volume per unit volume of adsorption bed. The over-all porosity, ϵ_0, is the sum of the internal and external porosities, i.e., $\epsilon_0 = \epsilon_i + \epsilon_e$. The over-all porosity gives the fractional volume of the adsorption bed accessible to molecules in the gaseous phase. Later in this paper the ratio of internal porosity to the over-all porosity, $\epsilon = \epsilon_i/\epsilon_0$, will be needed.

1.3. Composition of Feed

The gaseous mixture fed to the adsorption bed is assumed here to consist of carrier gases and adsorbates. This paper is restricted to a binary mixture of gases consisting of a carrier gas with a single adsorbate present at a much lower concentration.

1.4. Interparticle Flow Velocity

The carrier gas is assumed to flow in the interparticle spaces with an average linear velocity, $u = w/Q\epsilon_e$, where w represents the volumetric flow rate, and Q and ϵ_e are defined above. It should be noted that the average interparticle velocity, u, will always be greater than either the superficial velocity (the flow velocity calculated from the ratio w/Q), or the average flow velocity based on the over-all porosity (calculated from the ratio $w/Q\epsilon_0$). The interparticle flow velocity is used as the basic flow parameter because it leads to simpler equations.

1.5. Assumption of a Linear Isotherm

The adsorption process is limited to the region of a linear adsorption isotherm; i.e., the amount adsorbed at equilibrium is directly proportional to the concentration of adsorbate. The more general procedure of considering a nonlinear isotherm leads to severe mathematical difficulties, although solutions are available for special cases (*4–6*). In this paper we have ignored the problem of a nonlinear isotherm, and we justify this omission for two reasons. First, these equations are being developed for the design of systems to remove air contaminants. For this purpose, equations are needed which apply to the removal of diluted gases and vapors, and dilution generally removes any appreciable nonlinearity from an adsorption isotherm. Second, by developing a general solution for the linear case, we provide a basis of comparison for nonlinear cases.

1.6. Adsorption Mechanisms

In general it is useful to consider two types of adsorption; volumal adsorption and surface adsorption.

1.6.1. Volumal Adsorption. The equilibrium concentration of adsorbate in the narrow intraparticle pores, c_p, may be different from the adsorbate concentration in the interparticle spaces, c_e. Such an increase can be brought about by filling the pores with a compound in which the adsorbate is highly soluble or by van der Waals' forces originating at the pore surface. At equilibrium, the volumal equilibrium constant, K_c, may be defined as $K_c = c_p/c_e$. This equilibrium constant equals 1 if no volumal effects occur.

1.6.2. Surface Adsorption. The surface adsorption equilibrium constant is defined as

$$K_n = n/\epsilon_i c_p$$

where n represents the amount of adsorbate adsorbed on the surface per unit volume of pore space. For most untreated adsorbents, surface adsorption is more important than volumal adsorption.

1.7. The Rate of Mass Transfer

The over-all rate of mass transfer depends on the rates of several phenomena, and of these, the following are considered here:

1.7.1. Mass Transfer across a Film Surrounding the Adsorbent Grains. If mass transfer is controlled by a film surrounding the particles, then the constant H_c gives the rate of mass transfer per unit volume, per unit concentration difference across this film.

1.7.2. Mass Transfer across a Film on the Pore Walls. This is a mechanism analogous to the first mechanism described above, the only difference being the location of the film. It is assumed to proceed with a rate constant H_n.

1.7.3. Pore Diffusion. The adsorbate moves through the intraparticle pore structure by a process characterized by an effective diffusion coefficient D_i.

1.8. Interparticle Phenomena

Molecular diffusion of adsorbate in the interparticle spaces is important at low carrier gas velocities. We assume that the contribution of molecular diffusion to the movement of the gas along the bed may be characterized by an effective diffusion constant D.

A second interparticle phenomenon, "eddy diffusion," results from velocity differences in the flow through the bed packing. The best available description of this very complicated effect is found in Giddings' monograph (*3*). Here we assume that the over-all interparticle diffusion coefficient, D_g, may be expressed by the relationship

$D_g = D + Au$, where D is defined as above, A is the constant of eddy diffusion, and u is the interparticle velocity of the gas.

2. MATHEMATICAL ANALYSIS

The basic problem in dynamic adsorption is to describe the change of adsorbate concentration with time at a given point in the bed (usually at the bed exit), taking into account the experimental conditions and the known mechanisms of mass transfer. Previous mathematical solutions (*7–11*) of this problem have not been universally successful. Some appear oversimplified, and others are difficult to use because they are expressed in terms of integrals requiring the use of computers for their evaluation. In some of these equations the dimensionless groups are very complex and their physical meaning is difficult to interpret. As Kovach (*12*) recently stated, there is a real need for an improved method of analysis of adsorption beds.

Recently a new theory (*1*, *2*, *13*) of gas–solid chromatography was developed using the statistical moments of the breakthrough curve. This theory takes into account all mass transfer phenomena known to be important in dynamic adsorption and includes as special cases all previous solutions known to us. The aim of this paper is to show that this theory can be modified to derive simple expressions describing the adsorption capacity of a bed.

2.1. Definitions of the Statistical Moments

The breakthrough curves obtained following an injection of a very short pulse of adsorbate can be considered a type of probability distribution in concentration-time coordinates. The ordinary statistical moments are defined as

$$m_k' = \frac{\int_0^\infty c(\tau)\tau^k \, d\tau}{\int_0^\infty c(\tau) \, d\tau} \tag{1}$$

where m_k' is the kth ordinary statistical moment, $c(\tau)$ is the rate of breakthrough of adsorbate at time τ, τ is the time following the pulse input of adsorbate, and the central moments (about the mean) are defined as

$$m_k = \frac{\int_0^\infty c(\tau)(\tau - m_1')^k \, d\tau}{\int_0^\infty c(\tau) \, d\tau} \tag{2}$$

where m_k is the kth central moment. Because the first central statistical moment is equal to zero, we will drop the prime from m_1' and denote the first ordinary moment by m_1.

2.2. Gram-Charlier Series

The Gram-Charlier Series gives a general method for reconstructing a curve from its statistical moments. The general equation for these series is

$$c(t) = \sum_{k=0}^{\infty} c_k e^{-t^2/2} H_k(t) \tag{3}$$

where $H_k(t)$ = a Hermite polynomial; c_k = the frequency factor, a function of the statistical moments; $c(t)$ = the rate of breakthrough of adsorbate at the reduced central time, t; t = reduced central time, defined as $(\tau - m_1)/\sigma$; and $\sigma = \sqrt{m_2}$.

The elution curve following a pulse (delta function) input is described by the first three terms of a Gram-Charlier series as

$$c(t) = \left(\frac{1}{\sqrt{2\pi}} e^{-t^2/2}\right)\left[1 + \frac{m_3}{6\sigma^3}\{t^3 - 3t\} + \frac{1}{24}\left\{\frac{m_4}{\sigma^4} - 3\right\}\{t^4 - 6t^2 + 3\}\right] \tag{4}$$

2.3. The Meaning of the Statistical Moments

The first statistical moment gives the arithmetic mean holdup time for a pulse introduced at time $\tau = 0$. The second statistical moment, m_2, is called the variance and gives the sum of the squares of the deviations from the mean. The square root of m_2 is the standard deviation σ.

The third moment, m_3, furnishes information concerning the symmetry of the distribution curve. A positive value of the skewness coefficient, $S = m_3/\sigma^3$, indicates tailing of the distribution curve towards positive values of t.

The fourth statistical moment is a characteristic of the flattening of the distribution curve in comparison to the normal (Gaussian) distribution. The factor $E = (m_4/\sigma^4 - 3)$, usually called the coefficient of excess, can be positive, negative, or zero, with a positive value indicating that the distribution is flatter than the normal distribution, and a negative value indicating that the reverse is true.

The higher moments are less important because of the difficulty of determining their values experimentally. Generally it can be said that the higher even moments furnish more information about curve broadening and the higher odd moments further characterize the skewness.

2.4. Equations for the Statistical Moments

For the first moment, which defines the mean holdup time, the following equation is valid:

$$m_1 = \left(\frac{L + 2A}{u} + \frac{2D}{u^2}\right)(1 + \epsilon K_c[1 + K_n]) \tag{5}$$

where L is the length of the bed, and ϵ is the ratio ϵ_i/ϵ_e.

In the design of industrial adsorption beds, the terms $2A/u$ and $2D/u^2$ of Eq. (5) can be neglected because the factor L/u will be much greater than either $2A/u$ or $2D/u^2$. When the L/u factor dominates, the mean retention time is unaffected by the mechanisms influencing the rate with which adsorption equilibrium is established and the resulting equation for the first moment is

$$m_1 = \frac{L}{u}(1 + \epsilon K_c[1 + K_n]) \tag{6}$$

Further, if there is no volumal adsorption, $K_c = 1$ and Eq. (6) reduces to

$$m_1 = t_0(1 + \epsilon K') \tag{7}$$

where K' is the partition coefficient. This last expression is analogous to the equation commonly used in gas chromatography to describe the breakthrough time for the peak of the elution curve.

The expression for the second statistical moment, m_2, depends on the mechanism controlling mass transfer. Useful equations may be obtained by neglecting the higher powers of the term D/u, and assuming that only one mechanism of adsorption occurs, i.e., either volumal adsorption, where $K_c > 1$ and $K_n = 0$, or surface adsorption, where $K_n > 1$ and $K_c = 1$. This procedure can be easily adopted to the important cases of internal (pore) diffusion controlled mass transfer, where $H_c = \infty$, $H_n = \infty$, and $D_i < \infty$, and film controlled mass transfer, where either H_c and/or $H_n < \infty$ and $D_i = \infty$.

From derivations given earlier (*1*, *2*), we have for mass transfer characterized by the combined mechanisms of interparticle molecular and eddy diffusion, plus internal (pore) diffusion followed by surface adsorption:

$$\frac{m_2}{m_1^2} = \frac{1}{L}\left[\frac{2D}{u} + 2A + \frac{2(1 + K_n)^2R^2u}{15[1 + \epsilon(1 + K_n)^2]D_i}\right] \tag{8}$$

For interparticle molecular and eddy diffusion, plus internal (pore) diffusion followed by volumal adsorption:

$$\frac{m_2}{m_1^2} = \frac{1}{L}\left[\frac{2D}{u} + 2A + \frac{2\epsilon K_cR^2u}{15(1 + \epsilon K_c)^2D_i}\right] \tag{9}$$

For interparticle molecular and eddy diffusion, plus external film mass transfer resistance followed by volumal adsorption:

$$\frac{m_2}{m_1^2} = \frac{1}{L}\left[\frac{2D}{u} + 2A + \frac{2\epsilon^2K_cu}{H_c(1 + \epsilon K_c)^2}\right] \tag{10}$$

Usually either $K_n \gg 1$ or $K_c \gg 1$, so that the third term in the bracket on the right-hand side of Eqs. (8), (9), and (10) can be further simplified to give

$$\frac{2R^2u}{15\epsilon D_i}, \quad \frac{2R^2u}{15\epsilon K_cD_i}, \quad \text{or} \quad \frac{2u}{H_cK_c} \tag{11}$$

for Eqs. (8), (9), and 10), respectively.

Using these same procedures, simple expressions can be obtained for the skewness coefficient, $s = m_3/m_1^3$. Thus, for interparticle molecular and eddy diffusion, plus internal (pore) diffusion followed by surface adsorption, in the limiting case, $K_c = 1$, $K_n \gg 1$:

$$\frac{m_3}{m_1^3} = \frac{1}{L^2}\left[\frac{12D^2}{u^2} + \frac{24AD}{u} + 12A^2 + \frac{4DR^2}{5\epsilon D_i} + \frac{4AR^2u}{5\epsilon D_i} + \frac{4R^4u^2}{105\epsilon^2D_i^2}\right] \tag{12}$$

Similar expressions including volumal adsorption and/or film mass transfer resistance can be obtained.

We omit giving a general term for the fourth and higher statistical moments. The paper of Grubner (*1*) should be referred to for further expressions of this type.

2.5. Description of the Dynamic Adsorption Curve

It can be shown from the literature that the most important problem in dynamic adsorption concerns mass transfer controlled by intraparticle diffusion, and in this paper only this case is considered in detail.

First we seek an equation to describe the breakthrough curve following an unit step function input. Assuming a linear adsorption isotherm and first-order mass transfer kinetics, the relation between the elution curve following an unit pulse (delta function) input and the eluation curve following an unit step function (Heaviside function) input is the same as the relation between the probability density and probability distribution curves. Therefore, the desired equation can be readily obtained by integration of Eq. (4), yielding:

$$\frac{C}{C_0}(t) = \Phi(t) - \frac{S}{6}(t^2 - 1)\frac{e^{-t^2/2}}{\sqrt{2\pi}} + \frac{E}{24}(t^3 - 3t)\frac{e^{-t^2/2}}{\sqrt{2\pi}} \tag{13}$$

where $(C/C_0)(t)$ is the ratio of effluent to input concentration of adsorbate at the reduced central time, t; $\Phi(t)$ is the normal probability distribution curve, i.e.,

$$\Phi(t) = \frac{1}{\sqrt{2\pi}} \int_{-\infty}^{t} \exp\{-t'^2/2\} dt' \tag{14}$$

S is the skewness coefficient, m_3/σ^3; and E is the coefficient of excess, $m_4/m_2^2 - 3$.

If the excess term, E, is negligible, there is an approximate equation describing the breakthrough time for any given value of the concentration ratio C/C_0

$$\tau = m_1 \left\{ 1 + \frac{\sigma t_c}{m_1} + \frac{m_3}{6 m_2 m_1}(t_c^2 - 1) \right\} \tag{15}$$

where τ denotes the actual breakthrough time (same units as m_1) of the output concentration ratio corresponding to C/C_0, and t_c is the argument of the normal probability integral having a value equal to C/C_0. Stated in mathematical terms,

$$\frac{C}{C_0} = \frac{1}{\sqrt{2\pi}} \int_{-\infty}^{t_c} \exp\{-t_c'^2/2\}\, dt_c' \tag{16}$$

Both parameters are given in tables which are readily available (*14*).

2.6. Effective Adsorption Bed Capacity

The effective adsorption capacity of an adsorption bed in which there is ideal mass transfer is equal to

$$F^* = C_0 w m_1 \tag{17}$$

where C_0 is the input concentration, w is the volumetric flow through velocity, and m_1 is the first statistical moment. The next step is to introduce the ratio of actual to ideal adsorption capacity, F, defined as $F = F_a/F^*$, where F_a represents the actual capacity value obtained when only a specified degree of breakthrough is permitted.

From Eq. (15) it follows that

$$F = \tau/m_1 = 1 + \frac{\sigma t_c}{m_1} + 0.167(m_3/m_2m_1)(t_c^2 - 1) \tag{18}$$

2.7. Fractional Capacity Loss

The fractional capacity loss, M, which gives the fraction of the adsorption bed capacity loss because of the mechanisms of mass transfer present in any real adsorption bed, is

$$M \equiv 1 - F = -\frac{\sigma t_c}{m_1} + 0.167(m_3/m_2m_1)(1 - t_c^2) \tag{19}$$

We are most interested in the case of mass transfer controlled by mass transfer resistance, because mass transfer resistance is the controlling factor at the high carrier gas velocities that are of greater commercial interest. If we accept the simplification for mass transfer resistance controlled by internal (pore) diffusion (see Eqs. 11 and 12), then Eq. (15) can be rewritten in the form

$$\tau = m_1\left\{1 + \left(\frac{2R^2u}{15\epsilon D_iL}\right)^{1/2} t_c + \frac{R^2u}{21\epsilon D_iL}(t_c^2 - 1)\right\} \tag{20}$$

Defining ϕ as

$$\phi = \left(\frac{R^2u}{\epsilon D_iL}\right)^{1/2} \tag{21}$$

the equation for the fractional adsorption capacity becomes

$$F = 1 + a\phi t_c + b\phi^2(t_e^2 - 1) \tag{22}$$

and the equation for the fraction capacity loss becomes:

$$M = -a\phi t_c + b\phi^2(1 - t_e^2) \tag{23}$$

In the above equations, a and b are numerical constants having the values $a = (2/15)^{1/2} = 0.365$, and $b = 1/21 = 0.0477$.

2.8. Comparison of the Gram-Charlier and Gaussian Breakthrough Curves

It is assumed that the breakthrough curve can be adequately characterized by the first two terms of a Gram-Charlier series. A com-

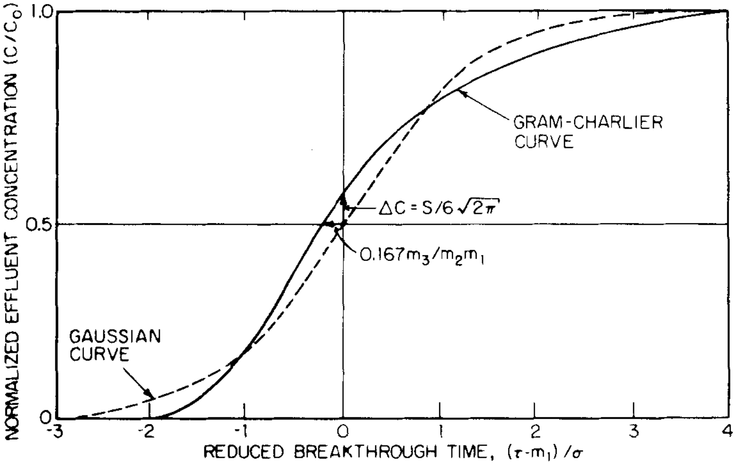

FIG. 2. Comparison of the Gram-Charlier and Gaussian breakthrough curves.

parison of the resulting Gram-Charlier curve with a Gaussian breakthrough curve is given in Fig. 2. It is particularly interesting to compare these two curves at the points $C/C_0 = 0.5$ and $\tau = m_1$. From Eq. (15) we find that at the point $C/C_0 = 0.5$ (i.e., $t_c = 0$)

$$\tau = m_1(1 - 0.167 m_3/m_2 m_1) \tag{24}$$

If the breakthrough curve were described exactly by a Gaussian curve, then τ would equal m_1 instead of $m_1(1 - 0.167 m_3/m_2 m_1)$ at the point $C/C_0 = 0.5$. Thus the factor $(1 - 0.167 m_3/m_2 m_1)$ gives the ratio of breakthrough times between the Gram-Charlier and the Gaussian curves at $C = 0.5C_0$ (see Fig. 2).

Similarity, from Eq. (13) we have at the time $\tau = m_1$ (i.e., $t = 0$)

$$C/C_0 = 0.5 + S/6\sqrt{2\pi} \tag{25}$$

indicating that at the point $\tau = m_1$, the breakthrough curve described by the Gram-Charlier series is somewhat higher than the normal probability curve, the difference being $\Delta C/C_0 = S/6\sqrt{2\pi}$.

3. THE FRACTIONAL LOSS OF ADSORPTION CAPACITY AS A FUNCTION OF MEASURABLE FACTORS

The practical value of the theory developed here is that it permits the design engineer to calculate M, the fractional loss of adsorption capacity, as a function of measurable factors, such as the size of the

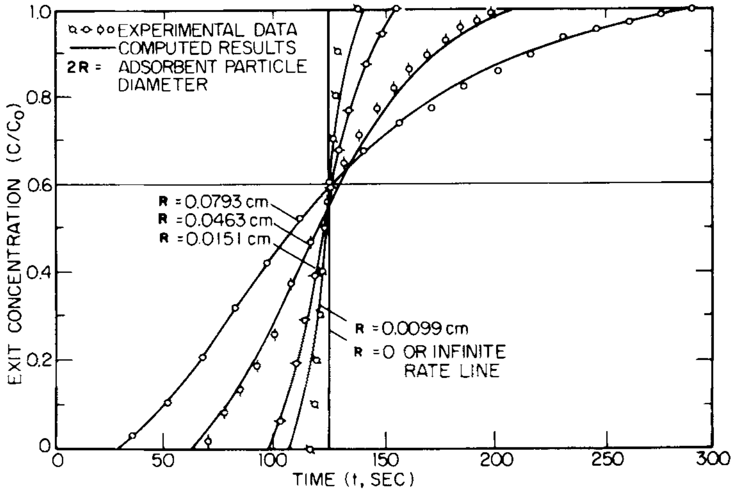

FIG. 3. The effect of adsorbent particle diameter on the breakthrough curves of Masamune and Smith (*11*).

adsorbent particles, the length of the adsorption bed, the flow velocity of the carrier gas, and the fractional interparticle void volume.

3.1. The Effect of Particle Radius

According to Eq. (23), the fractional capacity loss is a parabolic function of the particle radius, R, and can be rewritten in the simple form

$$M = a^*R + b^*R^2 \tag{26}$$

where a^* and b^* are factors independent of particle radius.

We wish to compare the above expression with experimental results already in the literature and for this purpose we begin with the nitrogen breakthrough curves described in the excellent paper of Masamune and Smith (*11*). The adsorbent was Vycor glass and the experimental conditions were maintained in the region of a well-defined linear adsorption isotherm. Figure 3, which is taken from their paper, shows the effect of the diameter of the adsorbent particle on the shape of the breakthrough curve. Using the experimental parameters given in their paper, namely, $u = 9.8$ cm/sec, $L = 2.25$ cm, $D_i = 4 \times 10^{-2}$/sec, we calculated the fractional capacity loss for representative values of R. Table 1 gives both the theoretical and experimental

TABLE 1

Comparison of Theoretical and Experimental Breakthrough Curves[a]

C/C_0	t_c	$(t_c^2 - 1)$	$+a\phi t_c$	$+b\phi^2(t_c^2 - 1)$	M_{calc}	M_{exp}	Experimental parameters	
0.05	−1.64	+1.69	−0.88	+0.17	+0.71	+0.66	$a = 0.365$	$\phi^2 = \frac{R^2 u}{\epsilon D_i L}$
0.1	−1.28	+0.64	−0.69	+0.07	+0.62	+0.59		
0.2	−0.84	−0.29	−0.45	−0.03	+0.48	+0.46	$b = 0.0477$	
0.4	−0.24	−0.94	−0.13	−0.10	+0.23	+0.24		$= \frac{6.24 \times 10^{-4}\ \text{cm}^2 \times 9.8\ \text{cm/sec}}{0.316 \times 4 \times 10^{-2}\ \text{cm}^2\text{/sec} \times 2.25\ \text{cm}}$
0.5	0.00	−1.00	0.00	−0.10	+0.10	+0.12	$\beta = 0.256$	
0.8	+0.84	−0.29	+0.45	−0.03	−0.42	−0.41	$\epsilon_i = 0.142$	
0.9	+1.28	+0.64	+0.69	+0.07	−0.76	−0.76		
							$\epsilon_e = 0.447$	$= 2.15$
							$\epsilon = 0.316$	$\phi = 1.47$
							$D_i = 4 \times 10^{-2}\ \text{cm}^2\text{/sec}$	$a\phi = 0.54$
							$L = 2.25\ \text{cm}$	$b\phi^2 = 0.103$
							$u = 9.8\ \text{cm/sec}$	
							$R = 7.9 \times 10^{-2}\ \text{cm}$	
0.05	−1.64	+1.69	−0.51	+0.06	+0.45	+0.42		
0.1	−1.28	+0.64	−0.40	+0.02	+0.38	+0.36	$R = 4.6 \times 10^{-2}\ \text{cm}$	
0.2	−0.84	−0.29	−0.26	−0.01	+0.27	+0.27		
0.4	−0.24	−0.94	−0.07	−0.03	+0.10	+0.11	$\phi = 0.85$	
0.5	0.00	−1.00	0.00	−0.03	+0.03	+0.05		
							$a\phi = 0.31$	
0.8	+0.84	−0.29	+0.26	−0.01	−0.25	−0.24		
0.9	+1.28	+0.64	+0.40	+0.02	−0.42	−0.41	$b\phi^2 = 0.035$	
0.05	−1.64	+1.69	−0.16	+0.007	+0.15	+0.19	$R = 1.5 \times 10^{-2}\ \text{cm}$	
0.1	−1.28	+0.64	−0.13	+0.002	+0.13	+0.15		
0.2	−0.84	−0.29	−0.08	−0.001	+0.08	+0.10	$\phi = 0.28$	
0.4	−0.24	−0.94	−0.02	−0.004	+0.02	+0.04		
0.5	0.00	−1.00	0.00	−0.004	0.00	0.00	$a\phi = 0.10$	
0.8	+0.84	−0.29	+0.08	−0.001	−0.08	−0.09	$b\phi^2 = 0.004$	
0.9	+1.28	+0.64	+0.12	+0.002	−0.12	−0.15		

[a] Based on data of Masamune and Smith (*11*).

values. The first and second columns of Table 1 list the C/C_0 and t_c values of the normal probability distribution, respectively, and the last two columns give the experimental and calculated values for the fractional capacity loss, M.

Table 2 gives the effect of particle radius on the fractional capacity loss, as predicted from Eq. (26) by assuming $a^* = 8.25$ and $b^* = 9.9$. The experimental results fit the theoretical parabolic equation.

TABLE 2

Effect of Particle Radius on the Fractional Capacity Loss[a]

Adsorbent particle radius, R (cm)	R^2	M/R	Fractional capacity loss, M_{theor}	Fractional capacity loss, M_{exptl}
0.079	61×10^{-4}	7.4	0.59	0.59
0.0463	21×10^{-4}	8.1	0.37	0.37
0.0151	2.3×10^{-4}	9.2	0.123	0.14
0.010	1.0×10^{-4}	8.4	0.082	0.084

[a] Based on data of Masamune and Smith (*11*).

The same dependence of the fractional capacity loss on particle radius is observed in experiments of Fultyn (*15*), who measured the breakthrough curves of sulfur dioxide on activated charcoal beds over a wide range of conditions. From his Fig. 37, we calculated at the breakthrough ratio, $C/C_0 = 0.1$, the experimental values shown in Table 3. These experimental values closely fit the theoretical parabolic equation.

TABLE 3

Effect of Particle Radius on the Fractional Capacity Loss[a]

Adsorbent particle radius, R (cm)	R^2	M/R	Fractional capacity loss, M_{theor}	Fractional capacity loss, M_{exptl}
0.03	9.0×10^{-4}	40.0	0.120	0.120
0.048	24.0×10^{-4}	29.0	0.140	0.140
0.070	49.0×10^{-4}	22.0	0.170	0.170

[a] Based on data of Fultyn (*15*).

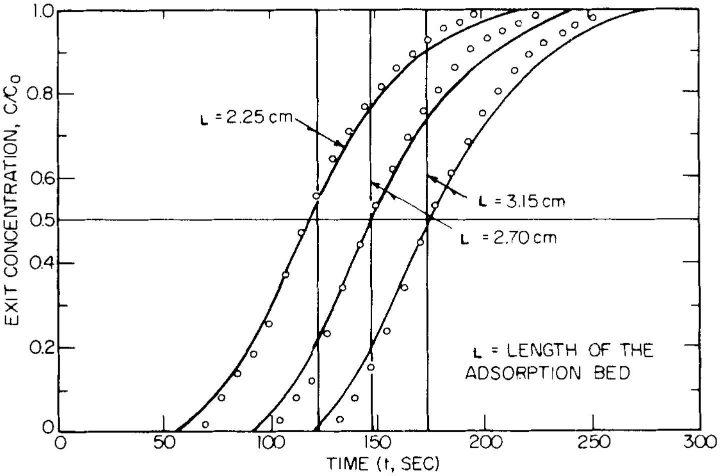

FIG. 4. The effect of bed length on the breakthrough curves of Masamune and Smith (*11*).

3.2. The Effect of Bed Length

The effect of bed length on the fractional capacity loss is seen in Fig. 4, taken from Ref. *11*. Numerical analyses of the effect of bed length can be obtained by rearranging Eq. (20) to give

$$M = a'(L)^{-1/2} + b'(L)^{-1} \tag{27}$$

Table 4 gives the theoretical and experimental fractional capacity losses vs bed length at $C/C_0 = 0.1$. Theoretical values for the fractional capacity losses observed by Masamune and Smith (*11*), were obtained by giving values of −52.6 and 163.0 to the constants a' and b', respectively. Again the experimental data closely fit the theoretical values.

TABLE 4

Effect of Bed Length on the Fractional Capacity Loss[a]

Bed length, L (cm)	Fractional capacity loss, M_{theor}	Fractional capacity loss, M_{exptl}
2.25	0.375	0.375
2.70	0.280	0.265
3.15	0.216	0.216

[a] Based on data of Masamune and Smith (*11*).

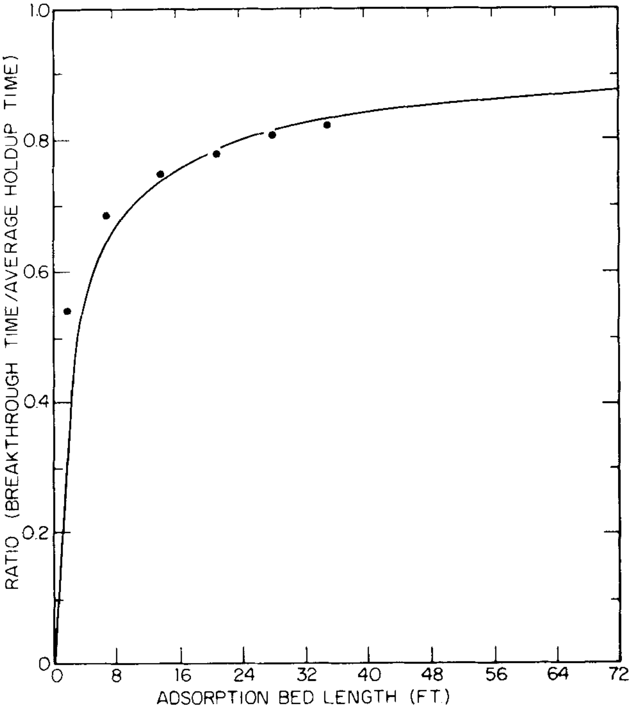

FIG. 5. The effect of bed length on capacity [from Browning (*16*)].

The predicted effect of bed length on adsorption bed capacity is supported by Browning's (*16*) study over a very wide range of values of the dynamic adsorption of krypton and xenon on activated charcoal beds. From Browning's plot of the change in bed capacity vs bed length (reproduced here as Fig. 5), values for the fractional capacity loss were found and compared with the theoretical values obtained by setting $a' = 2.2$ and $b' = 0.4$. The theoretical and experimental values are given in Table 5.

The effect of bed length on the fractional capacity loss also can be calculated from Fultyn's (*15*) experimental data. In Table 6 the fractional capacity losses at $C/C_0 = 0.1$ are compared with the theoretical values obtained by assuming $a' = 115.0$ and $b' = 150.0$.

3.3. The Effect of Carrier Gas Velocity

The effect of carrier gas velocity on the shape of breakthrough curves is rarely given in the literature, in sharp contrast to the vast

TABLE 5

Effect of Bed Length on the Fractional Capacity Loss[a]

Bed length, L (cm)	Fractional capacity loss, M_{theor}	Fractional capacity loss, M_{exptl}
2.2	0.47	0.47
7.2	0.32	0.32
14.5	0.25	0.26
21.5	0.20	0.21
29.5	0.18	0.19
35.0	0.17	0.17

[a] Based on data of Browning (*16*).

number of papers giving the so-called Height Equivalent of a Theoretical Plate (HETP) as a function of the carrier gas velocity. The shape of the breakthrough curve at a given carrier gas velocity is very important because it determines the efficiency of an adsorption bed at that particular velocity.

The mechanism controlling the shape of the breakthrough curve depends on the carrier gas velocity. At carrier gas velocities below 10 cm/sec, interparticle effects (molecular and eddy diffusion) must be taken into account. At carrier gas velocities greater than 10 cm/sec, intraparticle diffusion controls the establishment of equilibrium. Furthermore, if the carrier gas velocity is greater than 30 cm/sec, the flow will be at least partly turbulent and this must be taken into account.

Equation (28) gives the predicted effect of carrier gas velocity on the fractional capacity loss in the regime of internal (pore) diffusion:

TABLE 6

Effect of Bed Length on the Fractional Capacity Loss[a]

Bed length, L (cm)	Fractional capacity loss, M_{theor}	Fractional capacity loss, M_{exptl}
100	0.10	0.10
70	0.12	0.12
34	0.15	0.15

[a] Based on data of Fultyn (*15*).

$$M = a''(u)^{1/2} + b''u \tag{28}$$

The effect of carrier gas velocity on the shape of the breakthrough curve has been measured in some of the experiments of Fultyn (*15*). The breakthrough curves given in his Fig. 36 were normalized by us by assuming $m_1 = 100.0$ and the resulting values are listed in Table 7.

TABLE 7

Effect of Carrier Gas Velocity on the Fractional Capacity Loss[a]

Carrier gas velocity, u (cm/sec)	$u^{1/2}$	Fractional capacity loss, M_{exptl}	$M/u^{1/2}$
50	7.2	0.150	0.021
40	6.3	0.130	0.021
30	5.4	0.110	0.020
20	4.5	0.080	0.019

[a] Based on data of Fultyn (*15*).

In Table 7 the values of $m(u)^{-1/2}$ appear to be constant, indicating that in his experiments the first term on the right-hand side of Eq. (28) controlled the fractional adsorption capacity loss.

De Bruijn et al. (*17*) present considerable data on adsorption of low boiling gases at low temperatures on charcoal. The dependence of the point $C/C_0 = 0.1$ on the carrier gas velocity is found in their Fig. 11, which gives the breakthrough curve for the dynamic adsorption of methane on charcoal. In Table 8 values for the fractional capacity loss are listed and compared with values obtained from Eq. (28) by assuming $a'' = 0.022$ and $b'' = -0.002$.

TABLE 8

Effect of the Carrier Gas Velocity on the Fractional Capacity Loss[a]

Carrier gas velocity, u (cm/sec)	$u^{1/2}$	Fractional capacity loss, M_{exptl}	$M/u^{1/2}$	M/u
4.0	2.0	0.036	0.018	0.009
8.7	2.95	0.048	0.016	0.005

[a] Based on data of de Bruijn et al. (*17*).

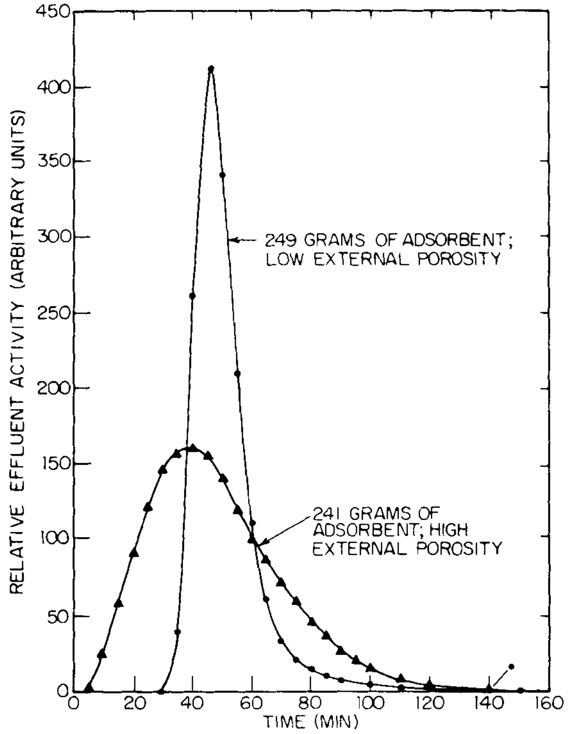

FIG. 6. The effect of external porosity on the broadening of breakthrough curves [from Browning (*16*)].

3.4. The Effect of External Porosity

Very little is known of the effect of external porosity on the performance of an adsorption bed. Browning's (*16*) finding that an increase in external porosity greatly diminishes the performance of an adsorption bed helps bridge this gap in our knowledge.

The breakthrough curves given in Browning's (*16*) Fig. 19 are reproduced here in Fig. 6. To analyze these curves we need to know the effect of porosity on the first and second statistical moments. From the definitions of porosity given in Section 1.2,

$$\epsilon = \frac{\epsilon_i}{\epsilon_e} = \frac{(1 - \epsilon_e)\beta}{\epsilon_e} \tag{29}$$

When internal (pore) diffusion controls mass transfer, the effect of the external porosity on the first and second statistical moments is given by:

$$\frac{dm_1}{m_1} = \frac{1}{\epsilon_e}\left(\frac{d\epsilon_e}{\epsilon_e}\right) \tag{30}$$

$$\frac{d(\phi^2)}{\phi^2} = \frac{d\epsilon}{(1 - \epsilon_e)\epsilon_e} = \frac{dm_2}{m_2} \tag{31}$$

$$\frac{d\phi}{\phi} = \frac{d\epsilon_e}{2(1 - \epsilon_e)\epsilon_e} = \frac{d\sigma}{\sigma} \tag{32}$$

From Eq. (30) it appears that the relative change of the first moment with external porosity is inversely proportional to the porosity, ϵ_e, and this effect is not great at high porosities. On the other hand, the effect of external porosity on the second moment, m_2, is proportional to $1/(1 - \epsilon_e)$, and this effect can become very strong at high porosities.

Both of these conclusions appear to be confirmed in the breakthrough curves given in Fig. 6. The average holdup times are nearly the same (the lower curve belongs to a bed containing slightly less adsorbent), but the porosities of the beds are quite different and as expected there is a great difference in the width of the curves.

The influence of the porosity ratio, ϵ, on the HETP (or, following our analysis, on the second moment, m_2) can be seen from experiments of Habgood and Hanlan (*18*). Figure 6 of their paper presents a series of HETP values for the dynamic adsorption of different hydrocarbons on charcoal. Keeping in mind that their HETP is approximately related to our m_2 by the equation

$$\text{HETP} \approx m_2 L/m_1^2 \tag{33}$$

it is seen that the slope of the HETP points, when plotted against carrier gas velocity, is proportional to ϕ^2 at higher velocities.

Habgood and Hanlan (*18*) examined adsorption on unactivated and activated charcoal. For both charcoals, the mercury and helium porosities are given, making it possible to calculate the porosity ratio, ϵ. From experiments with ethane at 100°C (Table 9), the ratio of HETP

TABLE 9

Effect of the Porosity Ratio, ϵ, on Curve Broadening[a]

	Density, Hg	Density, He	ϵ	HETP slope	Slope ratio	Porosity ratio
Activity 1.4	1.100	1.870	0.68	2.4	3.67	3.45
Activity 149	0.611	2.075	2.35	0.65		

[a] Based on data of Habgood and Hanlan (*18*).

slopes (or ϕ^2 values) is inversely proportional to the ϵ ratio, as required by Eq. (31). Similar results were obtained from analyses applied to the ten other compounds investigated by Habgood and Hanlan (*18*).

Independent but similar results for the effect of the porosity ratio on m_1 and m_2 (determined from pulses of carbon dioxide passing through columns containing activated charcoal, pumice, or glass beads) were reported in 1966 by Grubner and co-workers (*19*).

4. DISCUSSION OF THE RESULTS

First, let us discuss the theoretical model and its relationship to a real adsorption bed. The basic assumption is that the model operates in the region of a linear adsorption isotherm, with mass transfer controlled by first-order kinetics. The assumption of a linear adsorption isotherm is reasonable for most dynamic adsorption experiments performed at low concentrations. For some light gases, the linear range extends up to a gas concentration of at least several per cent (depending, of course, on the temperature) and for this reason it is a good model for many important problems, such as the recovery of radioactive fission gases. Of course the model still is applicable to heavier compounds at greater dilutions. The assumption of first-order kinetics seems plausible, especially for the case where the mass transfer rate is controlled by internal (pore) diffusion.

There is ample evidence in the literature for the importance of pore diffusion to adsorption chromatography and industrial gas adsorption. Nevertheless, with the exception of surface diffusion, our model accounts for all possible mechanisms of mass transfer. Even surface diffusion could probably be handled in a way similar to that used by Masamune and Smith (*11*). It is highly improbable that many mass transfer mechanisms could be important at the same time, but even this extreme case can be described by the statistical moments theory.

This theoretical model omits the change in gas velocity resulting from the pressure drop across the bed. This simplification is not always valid for gas chromatography, but it is generally quite acceptable for describing dynamic adsorption in industrial adsorbers. If necessary, the statistical moments can be modified to account for the effect of a pressure drop (*20*).

Two types of adsorption were considered: volumal and surface adsorption. Volumal adsorption is rather uncommon, but equations including volumal adsorption may be needed to describe "coated" adsorbents.

We should also discuss the limitations of the concepts used in the theory developed here. The definitions of the dimensions of the adsorption bed, as well as the definitions of the porosity, seem clear. Difficulties arise in the measurement of adsorbent particle size, especially if the adsorbent particles are irregular. We assumed that the particles are spherical, and the differences are adjusted for in the "effective diffusion coefficient." Nevertheless, if adsorbent particles of various diameters are present, one would expect that the larger particles will have a greater influence on the deviations from equilibrium than do the smaller ones.

The definitions of the various diffusion coefficients, including the eddy diffusion constant, have been given. The assumption that these coefficients are concentration independent is necessary for first-order kinetics.

The intraparticle diffusion constant is an empirical factor describing the effective combination of the various intraparticle mass transfer phenomena. The transport of adsorbate into the adsorbent particle can be very complex, especially if surface diffusion is present.

Usually pore diffusion is the most important mechanism of intraparticle mass transfer. It should be mentioned that the nature of pore diffusion depends on the diameter of the intraparticle pores. If these pores have a relatively large diameter (molecular mean free path of the molecules $\ll$ pore diameter), intraparticle mass transfer takes place by normal molecular diffusion. As the pores become narrower (molecular mean free path $\sim$ pore diameter) the character of the flow changes to Knudsen diffusion and the intraparticle diffusion coefficient must assume a value appropriate for Knudsen diffusion. In either case the pore diffusion coefficient is limited to a relatively narrow range of values. The smallest value is probably that of the Knudsen diffusion coefficient, which at ambient temperatures will not fall much below 0.01 cm^2/sec. On the other hand, in the absence of surface diffusion, the intraparticle diffusion coefficient cannot be greater than the bulk diffusion coefficient, the upper limit of which will be about 0.2 cm^2/sec.

We omit discussing the mass transfer rate constants, H_c and H_n, because the equations given here assume mass transfer is controlled by pore diffusion.

The equations used here for the statistical moments were derived using approximations described elsewhere (*1, 2*). We have found that these approximations are reasonable and the inaccuracies introduced by their use lie within the limits of experimental error.

The equation for the second statistical moment resembles the HETP equation, which was derived semiempirically for the case of gas chromatography by van Deemter et al. (*21*). It is a common error to assume that the HETP represents the bed length required to establish equilibrium. There is no discrete value for such a distance and therefore no such meaning for the HETP. It is the equation that has proved useful, not the concept, which has already been adequately criticized in the literature (*3*). The basic meaning of the HETP equation, and its relationship to the statistical moments, can be brought out in a very rough way by

$$\frac{m_2}{m_1^2} L = \text{HETP} = \left(\frac{\sigma}{Lu(K' + 1)}\right)^2 L = \frac{\sigma_x}{L} \tag{34}$$

where σ_x^2 is the variance of the breakthrough curve in units of length.

Basically the HETP concept describes a relationship between the first two moments of the breakthrough curve. From a rough approximation used in gas chromatography,

$$\sigma_x^2 = 2D_x\tau \tag{35}$$

then

$$D_x = \frac{D}{K' + 1} + \frac{Au}{K' + 1} + \frac{R^2u^2}{15\epsilon D_i(K' + 1)} \tag{36}$$

or

$$D_x = D_0 + D_1u + D_2u^2 \tag{37}$$

where D_x is the generalized diffusion constant. Thus the HETP equation can be considered an equation describing the dependence of a generalized diffusion constant on the carrier gas velocity.

The theory of statistical moments furnishes us, however, not only the equations for the first two moments, but also the equations for higher moments. These latter expressions are almost as important as the equation for the second moment. Especially interesting is the equation for the skewness of the breakthrough curve, from which it can be shown that the breakthrough curve is always positively skewed. This has the important consequence that C/C_0 values smaller than ½ are on the average nearer the mean than the corresponding C/C_0 values higher than ½, considerably increasing the effective adsorption capacity at low values of C/C_0.

Equation (13) is quite simple and can be used for a description of the breakthrough curve without the need for computer integrations. Calculating the statistical moments is somewhat tedious but can be performed on a desk calculator. We believe that it is important to realize that Eq. (13) can be further simplified to give expressions for the adsorption bed capacity and adsorption bed capacity loss.

From the qualitative point of view, all the basic relationships required by the theory appear fulfilled. The extensive data of Masamune and Smith (*11*) permit the quantiative agreement between theory and experiment to be examined. The results are satisfactory, even at low C/C_0 values, which are often difficult to predict. Yet these simple equations, because they include simultaneously the different phenomena affecting bed efficiency, appear to fulfill the requirements given by Kovach (*12*). Nevertheless, approximations were made, and the error introduced may not always lie within the experimental error.

5. FUTURE DEVELOPMENT OF THE THEORY

The theoretical expressions given here permit the efficiency of an adsorption bed to be related to experimental conditions. From an engineering standpoint, the value of the theory lies in its ability to recalculate the data from a given experiment to other conditions, allowing a design engineer to optimize the adsorption procedure. This theory may also prove useful in the measurement of mass transfer and equilibrium constants, especially for complicated systems, or at elevated temperatures, where classical adsorption methods meet with extreme difficulty. On the other hand, experimental work is needed to estimate the limits of validity of the equations developed here. If this report stimulates further investigations in this field, its purpose may be regarded as fulfilled.

Acknowledgments

This research reported upon in this document was supported in part by the National Aeronautics and Space Administration (Research Grant NGL 22-007-053) and by a contract with the American Iron and Steel Institute (Research Contract AISI-PFMC). We also gratefully acknowledge the thoughtful encouragement and assistance of the staff of the Department of Environmental Health Science, as well as the kind permission of W. E. Browning and of J. M. Smith to reproduce figures from their original paper.

List of Symbols

A	coefficient of eddy diffusion
a	constant = $\sqrt{2/15}$ ($\doteq$ 0.365)
a^*, a', a''	constants
b	constant = 1/21 ($\doteq$ 0.0477)
b^*, b', b''	constants
C	effluent concentration
C_0	input concentration
c_e	adsorbate concentration in the interparticle spaces
c	rate of breakthrough of adsorbate
c_k	frequency factor for a Hermite polynomial
c_p	adsorbate concentration in the intraparticle pores
D	coefficient characterizing the effect of interparticle molecular diffusion
D_g, D_x	over-all effective diffusion coefficients
D_i	coefficient of the diffusion in the pore space
D_0, D_1, D_2	constants for the over-all diffusion coefficient
E	coefficient of excess, $E = (m_4/m_2^2 - 3)$
F	ratio of actual to ideal adsorption bed capacity
F_a	actual adsorption bed capacity
F^*	ideal adsorption bed capacity
H_c, H_n	mass transfer rate constants
$H_k(t)$	Hermite polynomial
HETP	height equivalent of a theoretical plate
K'	partition coefficient
K_c, K_n	adsorption equilibrium constants
L	length of the adsorption bed
m_k'	ordinary statistical moments defined by Eq. (1)
m_k	central statistical moments defined by Eq. (2)
M	fractional loss of adsorption bed capacity
n	amount of adsorbate adsorbed on the surface of a unit volume of pore space
Q	cross sectional area of the bed
R	particle radius
S	skewness coefficient, $S = m_3/\sigma^3$
t	reduced central time, $t = (\tau - m_1)/\sigma$

t_c	argument of the normal probability curve having a value equal to C/C_0
t_0	breakthrough time of a gas chromatographic peak
u	interparticle linear velocity of the carrier gas
w	volumetric flow rate
β	porosity of the adsorbent particle
ϵ	ratio of the internal and external porosity, $\epsilon = \epsilon_i/\epsilon_e$
ϵ_e	external porosity
ϵ_i	internal porosity, $\epsilon_i = \beta(1 - \epsilon_e)$
ϵ_0	over-all porosity, $\epsilon_0 = \epsilon_i + \epsilon_e$
σ	standard deviation, $\sigma = \sqrt{m_2}$
σ_x	standard deviation in units of length
τ	actual breakthrough time
ϕ	modulus defined as $\phi = \left(\frac{R^2u}{\epsilon D_iL}\right)^{1/2}$
$\Phi(t)$	normal probability curve for the argument, t

REFERENCES

1. O. Grubner, "Statistical Moments Theory of Gas-Solid Chromatography," in *Advances in Chromatography,* Vol. 6, Dekker, New York, 1968, p. 173.
2. E. Kučera, "Contribution to the Theory of Chromatography," *J. Chromatogr.,* **19,** 237 (1965).
3. J. C. Giddings, *The Dynamics of Chromatography, Part I: Principles and Theory,* Dekker New York, 1965.
4. R. H. Perry, ed., *The Chemical Engineers' Handbook,* 4th ed., McGraw-Hill, New York, 1963.
5. G. J. Krige and V. Pretorius, "Frontal Analysis Chromatography: Theoretical Treatment of Stationary Front Widths Neglecting Radial Permeability Fluctuations," *Anal. Chem.,* **37,** 1195 (1965).
6. K. R. Hall, L. C. Eagleton, A. Acrivos, and T. Vermeulen, "Pore- and Solid-Diffusion Kinetics in Fixed Bed Adsorption Under Constant-Pattern Conditions," *Ind. Eng. Chem. Fundam.,* **5,** 212 (1966).
7. O. A. Hougen and W. R. Marshall, "Adsorption From a Fluid Stream Flowing Through a Stationary Granular Bed," *Chem. Eng. Progr.,* **43,** 197 (1947).
8. L. Lapidus and N. G. Amundson, "Mathematics of Adsorption in Beds VI: The Effect of Longitudinal Diffusion in Ion Exchange and Chromatographic Columns," *J. Phys. Chem.,* **56,** 984 (1952).
9. J. B. Rosen, "General Numerical Solution for Solid Diffusion in Fixed Beds," *Ind. Eng. Chem.,* **46,** 1590 (1964).
10. J. C. Giddings and H. Eyring, "A Molecular Dynamic Theory of Chromatography," *J. Phys. Chem.,* **59,** 416 (1955).
11. S. Masamune and J. M. Smith, "Adsorption Rate Studies—Significance of Pore Diffusion," *Amer. Inst. Chem. Eng. J.,* **10,** 246 (1964).

12. J. L. Kovach, "Adsorbents; Review and Projection," in *Proceedings of the Tenth USAEC Air Cleaning Conference,* New York City, August, 1968. Harvard Air Cleaning Laboratory, Boston, CONF-680821, p. 149 (December, 1968).
13. D. A. McQuarrie, "On the Stochastic Theory of Chromatography," *J. Chem. Phys.,* **38,** 437 (1963).
14. R. O. Weast, ed., *Handbook of Chemistry and Physics,* 49th ed., Chemical Rubber Publishing Company, Cleveland, Ohio, 1968.
15. R. V. Fultyn, "Adsorption of Sulfur Dioxide in Fixed and Fluidized Carbon Beds." Thesis submitted in partial fulfillment of the requirements for the degree of Doctor of Science, Harvard School of Public Health, Boston, Massachusetts, 1960.
16. W. E. Browning, R. E. Adams, and R. D. Ackley, *Removal of Fission Product Gases from Reactor Off-Gas Streams by Adsorption,* United States Atomic Energy Commission Report, ORNL 59-6-47, Oak Ridge National Laboratory, Oak Ridge, Tennessee, June, 1959.
17. H. de Bruijn, A. Grutter, E. Romberg, B. A. Shorrock, L. Werner, and F. C. Wood, "Removal of Fission-Product Noble Gases From the Helium of a High-Temperature Gas-Cooled Reactor Using Charcoal at Low Temperature," *Trans. Inst. Chem. Eng.,* **42,** 365 (1964).
18. H. W. Habgood and J. F. Hanlan, "A Gas Chromatographic Study of the Adsorptive Properties of a Series of Activated Charcoals," *Can. J. Chem.,* **37,** 843 (1959).
19. O. Grubner, M. Ralek, and A. Zikanova, "Calculation of the Mass Transfer Coefficients by Means of a More Exact Theory of Gas-Solid Chromatography, Part I: Comparison of Columns Charged With Glass Spheres and Materials of High Internal Porosity," *Collect. Czech. Chem. Commun.;* **31,** 852 (1966). O. Grubner, M. Ralek, and E. Kučera, "Calculation of the Mass Transfer Coefficients by Means of a More Exact Theory of Gas-Solid Chromatography, Part II: Variance and Assymetry of the Chromatographic Curves in the System Carbon Dioxide-Activated Charcoal," *Ibid.,* **31,** 2629 (1966).
20. D. Underhill, "Calculation of the Pressure Drop Effect in Gas Chromatography," *Separ. Sci.,* **5,** 219 (1970).
21. J. J. van Deemter, F. J. Zuiderweg, and A. Klinkenberg, "Longitudinal Diffusion and Resistance to Mass Transfer as Causes of Nonideality in Chromatography," *Chem. Eng. Sci.,* **5,** 271 (1956).

Received by editor March 10, 1970